

<https://helda.helsinki.fi>

Anatomic and MRI bases for pontine infarctions with patients presentation

Vlas, Tatjana

2022-08

Vlas , T , Brkic , B G , Stevic , Z , Vukic , M , Durovic , O , Kostic , D , Stanisavljevic , N , Marinkovic , I , Kapor , S & Marinkovic , S 2022 , ' Anatomic and MRI bases for pontine infarctions with patients presentation ' , Journal of Stroke & Cerebrovascular Diseases , vol. 31 , no. 8 , 106613 . <https://doi.org/10.1016/j.jstrokecerebrovasdis.2022.106613>

<http://hdl.handle.net/10138/346801>

<https://doi.org/10.1016/j.jstrokecerebrovasdis.2022.106613>

cc_by_nc_nd

publishedVersion

Downloaded from Helda, University of Helsinki institutional repository.

This is an electronic reprint of the original article.

This reprint may differ from the original in pagination and typographic detail.

Please cite the original version.

Anatomic and MRI Bases for Pontine Infarctions with Patients Presentation

Tatjana Vlašković, MD,^a Biljana Georgievski Brkić, MD, PhD,^b
Zorica Stević, MD, PhD,^c Marjana Vukićević, MD, PhD,^d Olivera Đurović, MD,^e
Dejan Kostić, MD, PhD,^f Nataša Stanisavljević, MD, PhD,^g
Ivan Marinković, MD, PhD,^h Slobodan Kapor, MD, PhD,ⁱ and
Slobodan Marinković, MD, PhD^j

Objectives: There are scarce data regarding pontine arteries anatomy, which is the basis for ischemic lesions following their occlusion. The aim of this study was to examine pontine vasculature and its relationships with the radiologic and neurologic features of pontine infarctions. *Materials and methods:* Branches of eight basilar arteries and their twigs, including the larger intrapontine branches, were microdissected following an injection of a 10% mixture of India ink and gelatin. Two additional brain stems were prepared for microscopic examination after being stained with luxol fast blue and cresyl violet. Finally, 30 patients with pontine infarctions underwent magnetic resonance imaging (MRI) in order to determine the position and size of the infarctions. *Results:* The perforating arteries, which averaged 5.8 in number and 0.39 mm in diameter, gave rise to paramedian and anteromedial branches, and also to anterolateral twigs (62.5%). The longer leptomeningeal and cerebellar arteries occasionally gave off perforating and anterolateral twigs, and either the lateral or posterior branches. Occlusion of some of these vessels resulted in the paramedian (30%), anterolateral (26.7%), lateral (20%), and combined infarctions (23.3%), which were most often isolated and unilateral, and rarely bilateral (10%). They were located in the lower pons (23.3%), middle (10%) or rostral (26.7%), or in two or three portions (40%). Each type of infarction usually produced characteristic neurologic signs. The clinical significance of the anatomic findings was discussed. *Conclusions:* There was a good correlation between the intrapontine vascular territories, the position, size and shape of the infarctions, and the type of neurologic manifestations. **Key Words:** Acute pontine infarction—Pontine arteries anatomy—Basilar artery—Occlusive cerebrovascular disease—Neurologic signs
© 2022 The Authors. Published by Elsevier Inc. This is an open access article under the CC BY-NC-ND license (<http://creativecommons.org/licenses/by-nc-nd/4.0/>)

From the ^aUniversity of Belgrade, Faculty of Medicine, Laza Lazarević Hospital of Psychiatry, Faculty of Medicine, University of Belgrade, Belgrade, Serbia; ^bUniversity of Belgrade, Faculty of Medicine, Sveti Sava Stroke Hospital, Department of CT and MRI, Belgrade, Serbia; ^cClinic of Neurology, Clinical Center of Serbia, School of Medicine, University of Belgrade, Belgrade, Serbia; ^dUniversity of Belgrade, Faculty of Medicine, Sveti Sava Stroke Hospital, Department of Neurology, Belgrade, Serbia; ^eUniversity of Belgrade, Faculty of Medicine, Sveti Sava Stroke Hospital, Department of Neurology, Belgrade, Serbia; ^fMilitary Medical Academy, Institute of Radiology, Belgrade, Serbia; ^gUniversity of Belgrade, Clinical Hospital Center Bezanijska Kosa, Department of Hematology, Belgrade, Serbia; ^hUniversity of Helsinki, Helsinki University Hospital, Clinical Neuroscience, Neurology, Helsinki, Finland; ⁱUniversity of Belgrade, Faculty of Medicine, Institute of Anatomy, Department of Neuroanatomy, Belgrade, Serbia; and ^jUniversity of Belgrade, Faculty of Medicine, Institute of Anatomy, Department of Neuroanatomy, Belgrade, Serbia.

Received May 8, 2022; revision received June 10, 2022; accepted June 19, 2022.

Corresponding author. E-mail: ivan.marinkovic@hus.fi.

1052-3057/\$ - see front matter

© 2022 The Authors. Published by Elsevier Inc. This is an open access article under the CC BY-NC-ND license

(<http://creativecommons.org/licenses/by-nc-nd/4.0/>)

<https://doi.org/10.1016/j.jstrokecerebrovasdis.2022.106613>

Introduction

Pontine infarctions (PIs) are rare events since they account for only about 7% of all ischemic strokes (IS) of the brain.^{1–4} The PIs can be positioned in the caudal (lower) pons, middle or rostral (upper) pons, or in two or three of these portions, as well as in the paramedian, anterolateral, lateral, or posterior region, including their various combinations.^{1–5} Atheromatous plaques of the basilar artery (BA) and small vessel disease are the most frequent cause of ischemic lesions.^{1–8} Clinical manifestations mainly comprise certain lacunar syndromes.^{1, 3, 7, 9}

Since there is a relatively low incidence of the PIs, we decided to examine them in detail, especially related to their radiologic location and size, and anatomic bases for the symptoms they produce. In order to do this, we first made an anatomic study of the BA branches, since there are rare reports on this subject.^{10–12} Thereafter, the obtained data were compared with radiologic and clinical characteristics of the patients we enrolled. Only a few similar studies have been reported thus far.^{2, 7–9, 12}

Methods

Anatomic examination

Eight brain stems, with their 16 right and left sides, respectively, were provided from a routine autopsy with the permission of the authorities of the Institute of Pathology. Vertebral (VA) and basilar arteries of each brain stem were injected with a 10% mixture of India ink and gelatin, and fixed in 10% formaldehyde solution for 3 weeks. Thereafter, a microdissection of the superficial BA branches and their larger intrapontine twigs was performed under a stereo-microscope.

Two additional brain stems were provided, and blocks of the pons were cut off in transverse sections. They were prepared for a histologic examination and stained with luxol fast blue and cresyl violet.¹³ The pontine structures were microscopically identified, based on our knowledge and on data from specific publications.^{10,12,14} The slices were used for making schematic presentations with the addition of the intrapontine arteries drawings.

Patient examinations

Thirty patients with pontine infarctions were enrolled in two years (from March 2018 to April 2020) at our Stroke Hospital. Personal and family medical histories were first obtained for each of them, and then general and neurologic examinations were performed, as well as the necessary biochemical analyses. In addition to the magnetic resonance imaging (MRI), most of the patients underwent MRI angiography (MRA). Written consent was provided from all patients or their relatives, which was approved by the Ethics Committee of the Clinical center.

Radiologic examination

Pontine infarctions and intracranial arteries were studied by MRI techniques, whilst the neck vessels were explored by ultrasonography.

The examination was carried out via MRI machine General Electric, Signa HdX 1.5T. The corresponding procedures were applied to provide T1-weighted, T2-weighted, diffusion-weighted (DWI), and fluid-attenuated inversion recovery (FLAIR) images. A brain MRA (3D TOF) was performed in 21 patients.

Accordingly, the following sequences and procedures were applied. T1-weighted: TR/TE 450/min ms, matrix 320 × 224, FOV 24, slice thickness 5 mm, spacing 0.5mm. T2-weighted: TR/TE 4600/108 ms, matrix 384 × 256, FOV 24, slice thickness 5 mm, spacing 0.5 mm, as well as TR/TE (450/min), matrix 256 × 192. T2-fat saturation: TR/TE (4600/102), matrix 384 × 256, FOV 26, slice thickness (3 mm), spacing 1mm. DWI: TR/TE (ms) 8000/min, matrix 128 × 128, FOV 24, slice thickness (5 mm), spacing (0.5 mm), b-values, 0 s/mm² and 1000 s/mm². FLAIR: TR/TE 8000/120 ms, matrix 256 × 192, FOV 24, slice thickness 5 mm, spacing 0.5 mm, TI (2000 ms).

Brain MRA (3D TOF): TR/TE (23/7), matrix 384 × 224, FOV (22), section thickness 2 mm, overlap lochs 10, lochs per slab 32, FA 20°, acquisition time 5min 4s. Neck MRA (TRICKS): TE minimum, matrix 320 × 192, FOV 36.0, PHASE FOV 0.75, section thickness 3.2 mm, scan lochs 28, FA 30°, output temporal phases 15, scan time 1.10 (0.15).

Atherosclerosis of the BA was diagnosed indirectly, by using standard MRI sequences, i.e. T1- and T2-weighted, including the MRA. A precise BA plaque diagnosis can be made by applying multicontrast black blood sequences, postcontrast T1-weighted images, contrast-enhanced MRA, and postgadolinium wall contrast enhancement.⁶ We did not use these procedures, since our main goal was a correlation of the anatomic results, MRI findings, and neurologic signs. In spite of this, we managed to diagnose many types of vascular pathology, e.g. irregular lumen, stenosis, occlusion, tortuosity, angulation, dissection, and hypoplasia.

Ultrasonography (US) was performed in 14 patients by using Canon Inc Tus AI600 (APLIO I 600) apparatus for examination of the cervical arteries, i.e. both vertebral (VAs), internal carotid (ICAs) and the common carotid arteries (CCAs), including the subclavian arteries.

Statistical analysis

Methods of descriptive and analytical statistics were implemented using SPSS statistical analysis software, Version 20.0 (SPSS, Chicago, Illinois, USA). Patient features, and MRA and US findings, were analyzed using methods of descriptive statistics. Numerical variables were expressed as a mean ± SD (standard deviation) in the case of normal distribution, or median (interquartile range) if variables did not follow normal

distribution, and as percentages for categorical data. The percentages and frequencies of pontine infarctions were compared using chi-square and Fisher's exact test. For analysis of pontine infarct size, the Student t test and Mann Whitney U test were applied. Correlations between parameters were analyzed using Spearman's correlation test.

Results

Anatomic study

The BA gives rise to the perforating and leptomeningeal side branches (Figs. 1 and 2). Three main groups of branches can be distinguished: the perforating, pontine leptomeningeal, and cerebellar.

Perforating arteries

These arteries (PerfAs) (Figs. 1 and 2) ranged in number from 4 to 10 unilaterally (5.8 on average), and between 0.09 mm to 0.81 mm in diameter (mean, 0.39 mm). They were divided into the caudal group, entering the foramen caecum, the middle group, penetrating the edges of the basilar groove, and the rostral group, which entered the most caudal part of the interpeduncular fossa (Fig. 2).

Some of them always arose from the BA, either separately or by their own common trunks, or by common stems with some of the BA leptomeningeal vessels (Fig. 2). The PerfAs gave off 1–3 anterolateral twigs in 62.5% (Fig. 2). In one specimen, a caudal PerfA supplied both the ipsilateral and contralateral paramedian region of the pons. Another one nourished the upper part of the medullary pyramid and the olive.

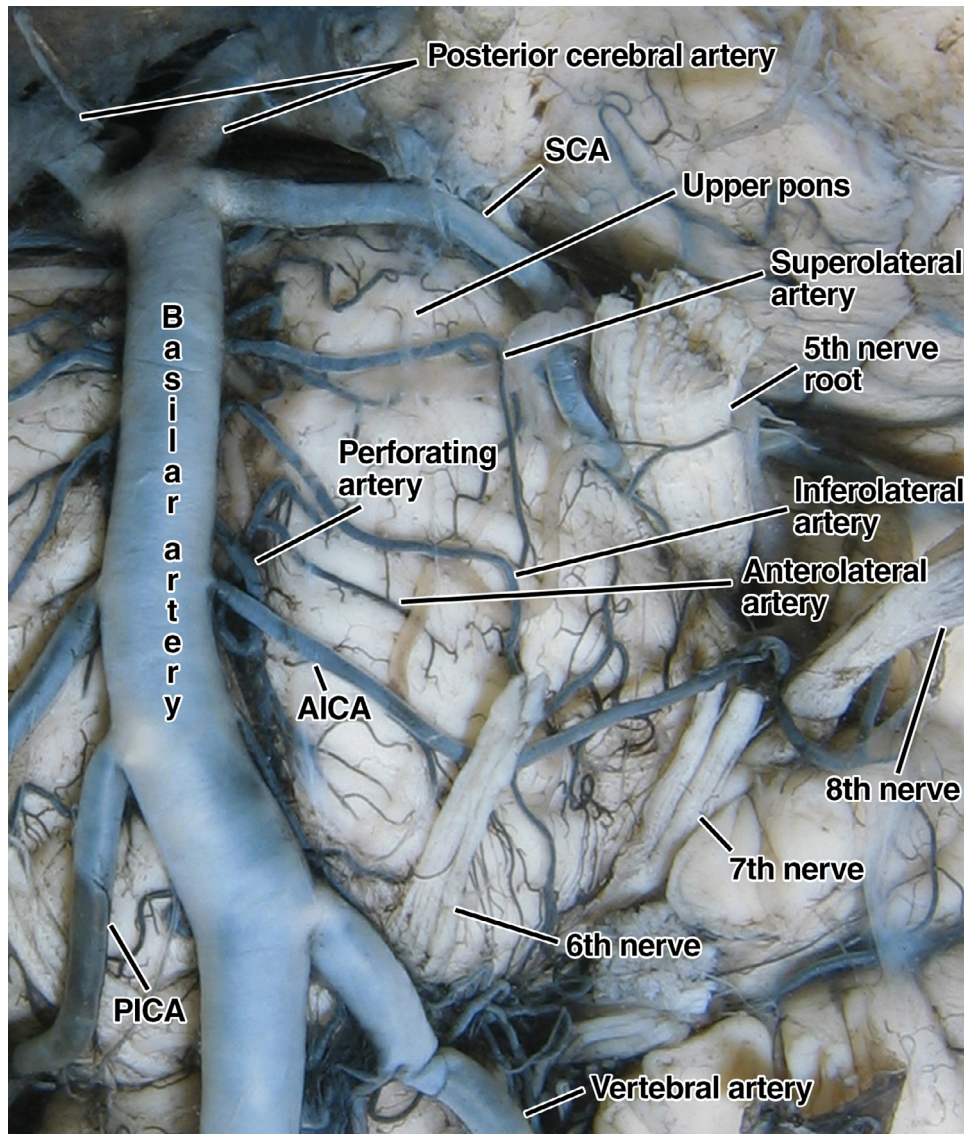


Fig. 1. Anterior view of dissected pontine arteries in a specimen

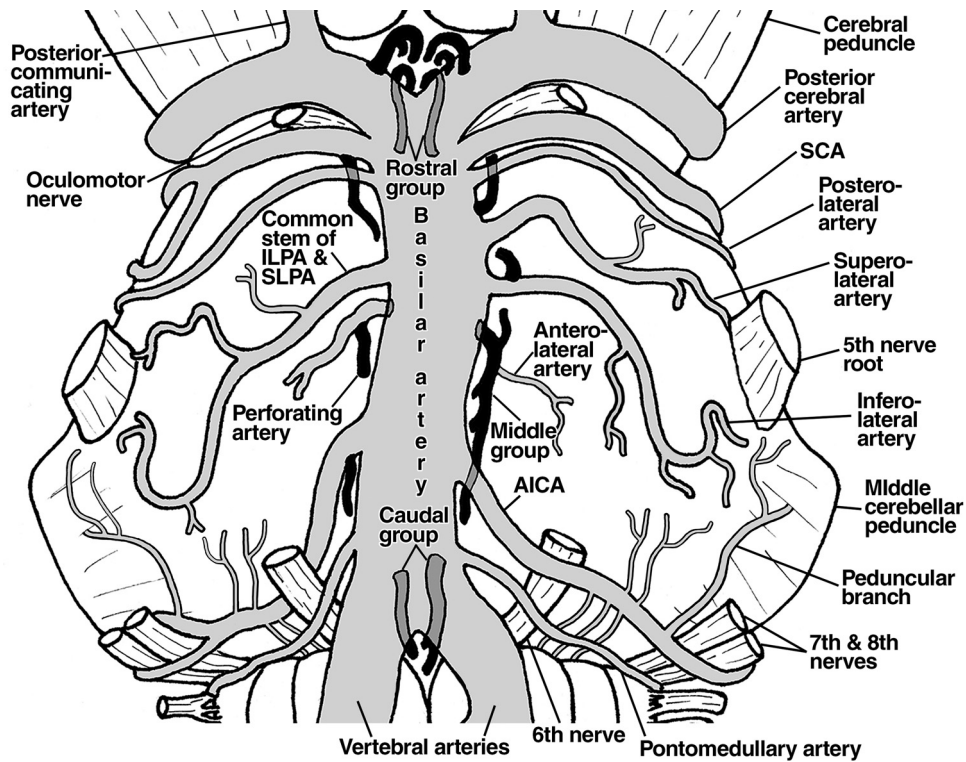


Fig. 2. A schematic presentation of the basilar artery, perforating (black), anterolateral, lateral, and cerebellar arteries. Note three groups of the perforators: caudal, middle and rostral. Also note a common trunk of the perforators, which gives rise to an anterolateral artery, and a common stem of the ILPA and SLPA

Leptomeningeal arteries

They comprise the short pontomedullary (PMA) and anterolateral arteries (ALAs), then the long inferolateral pontine artery (ILPA), superolateral (SLPA) and postero-lateral (PLPA), as well as some branches of the cerebellar arteries (Figs. 1 and 2), i.e. of the anterior inferior

cerebellar artery (AICA) (Fig. 3), the superior cerebellar artery (SCA) and, in only one case, the posterior inferior cerebellar artery (PICA) (Fig. 1).

The short ALAs were multiple vessels, 4-8 (mean, 5.2) in number on each side. They arose directly from the BA or from its PerfAs, and less frequently from the long

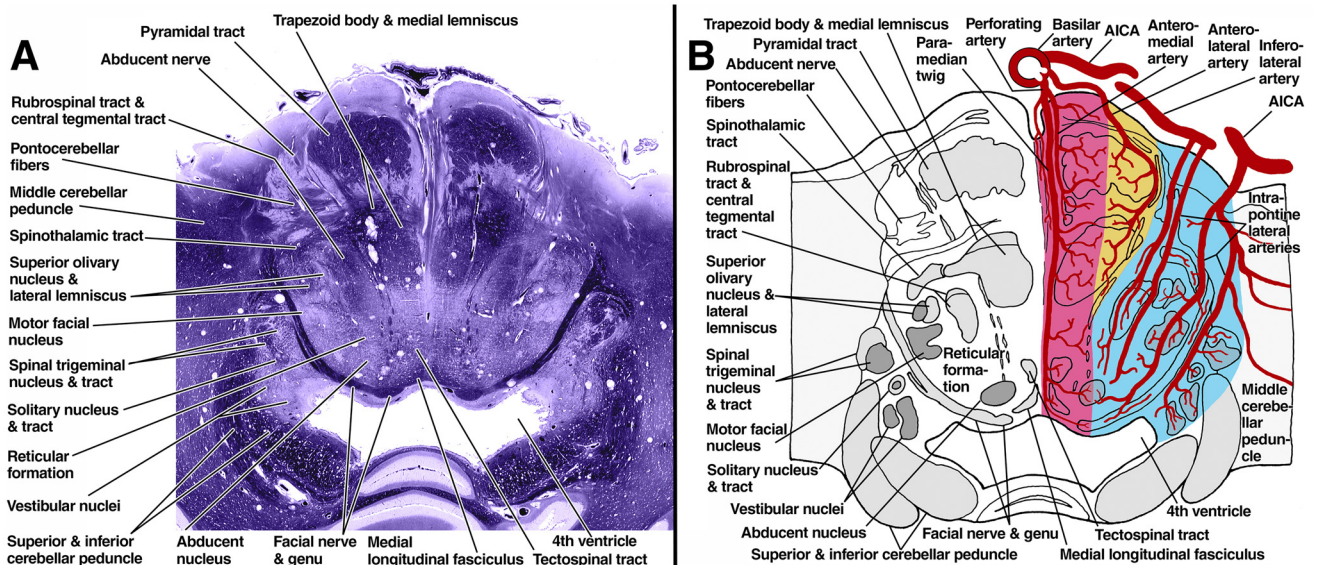


Fig. 3. Transverse section of the lower pons (A) and a similar drawing (B). Note the paramedian (pink), anterolateral (yellow), and lateral vascular territory (blue)

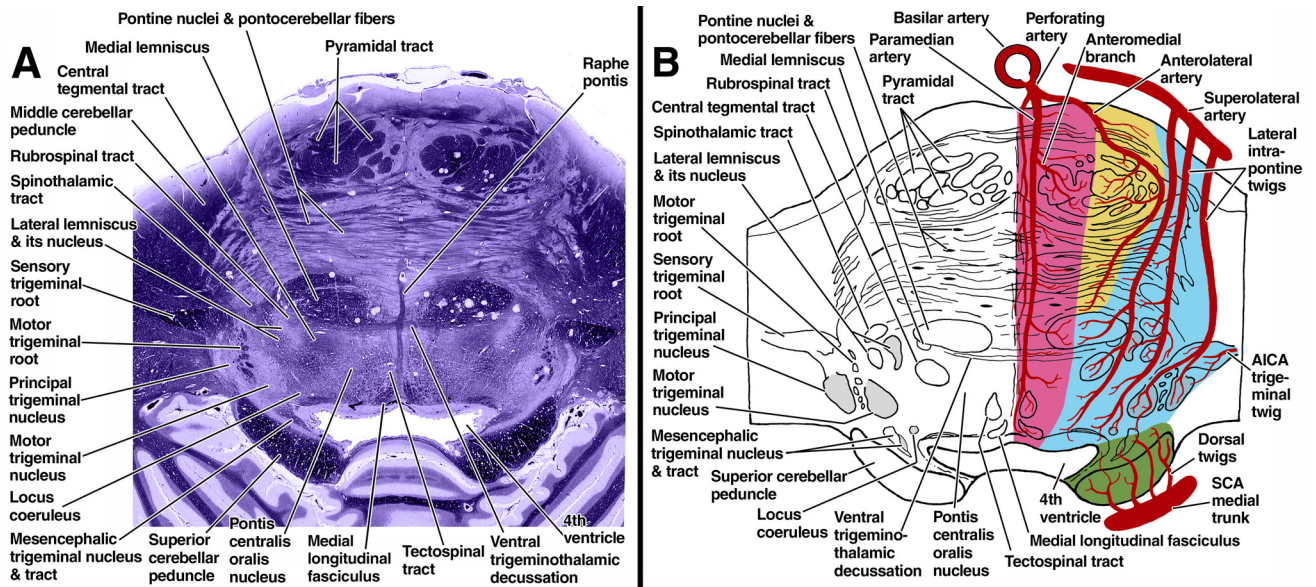


Fig. 4. Transverse section of the middle pons (A) and a similar drawing (B). Note the paramedian (pink), anterolateral (yellow), lateral (blue), and posterior (dorsal) vascular territory (green)

leptomeningeal or cerebellar arteries (Fig. 2). The PMA is also a short branch of the BA, which terminated superior to the medullary olive (Fig. 2).

The ILPA, which was always singular, ran inferiorly and laterally, and ended just below the level of the trigeminal nerve root (Fig. 2). It can give rise to the ALAs, rarely to a single PerfA, and always to lateral intrapontine branches.

The SLPA, which arose separately in all cases but one (Fig. 2), usually gave off 1 or 2 ALAs and rarely

to a PerfA, but always to lateral twigs. It terminated at the level of the trigeminal nerve root (Fig. 2). The PLPA arose just below the origin site of the SCA (Fig. 2), and it ended above the trigeminal nerve root.

As already mentioned, some branches of the AICA and SCA also took part in supplying certain regions of the pons. The AICA mainly gave off twigs to the lateral part of the lower pons (Fig. 3B), and the SCA to the most posterior (dorsal) part of the rostral tegmentum (Figs. 4B and 5B).

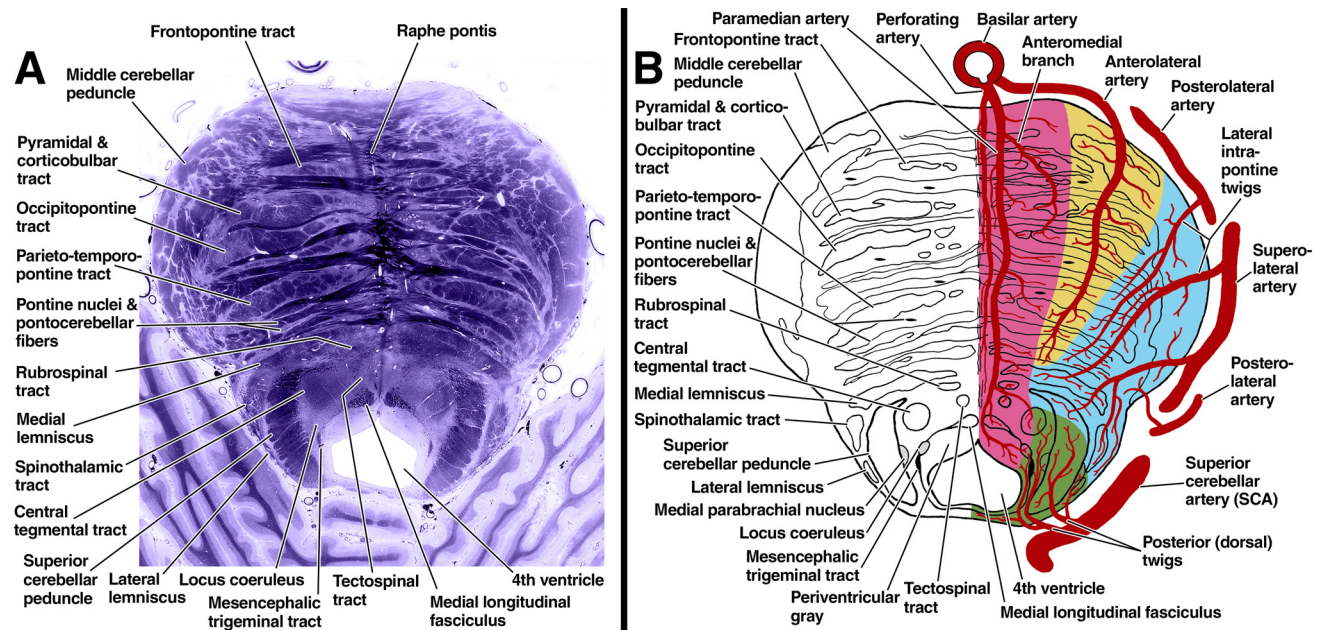


Fig. 5. Transverse section of the rostral pons (A) and a similar drawing (B). Note the paramedian (pink), anterolateral (yellow), lateral (blue), and posterior (dorsal) vascular territory (green)

Some PerfAs and ALAs also can arise from the cerebellar arteries (Fig. 2).

Anastomotic channels

Anastomoses between the neighboring PerfAs were present in 25% of the right and/or left halves of the brain stem, with a mean diameter of 0.14 mm. Anastomoses were seen among the SLPA and ILPA branches in 56.3%, usually close to the trigeminal nerve root. They ranged 1–3 in number, and averaged 0.13 mm in diameter.

Vascular territories

On the basis of our microdissection, and the examination of a few authors,^{10, 12} three drawings of the lower, middle and rostral pontine sections were made with inserted intrapontine vessels (Figs. 3B through 5B). They are among the most precise drawings of the intrapontine vasculature ever designed. Nevertheless, there is a certain variability of the extent of the corresponding vascular territories in some specimens. In any case, the lateral territory was the largest one in the lower and middle pons (Figs. 3B and 4B), whilst the anterolateral region usually was the smallest one at all levels (Figs. 3B through 5B).

Patient examinations

The 30 enrolled patients ranged between 44 and 84 years of age (mean, 63.7±10.35). The females' mean age (69) was significantly higher than that of the males (60) ($p=0.012$). In all patients, the MRI location and size of the infarctions were examined, with a determination of the affected vascular territory and the lesioned pontine structures in those regions.

Infarction characteristics

The risk factors

The ischemic lesions occurred as a consequence of certain predisposing influences (Table 1). A high statistical significance was observed in patients with arterial hypertension, obesity and alcohol abuse ($p<0.001$ each), including dyslipidemia ($p=0.006$). Two, three or more risk factors were present in 83.4% of the patients (Table 1).

Arteries pathology

Due to the mentioned factors, certain alterations occurred which involved cranial, cervical or both segments of certain arteries in 86.7%. Various types of pathology and anatomic variants were present, particularly irregular lumen, stenosis, occlusion, elongation, angulation, tortuosity and hypoplasia, and very rarely fenestration and dissection. The BA atherosclerosis and small

Table 1. Vascular risk factors in pontine infarctions

Risk factors: n/% (p=)	Combinations: n/% (p=)
Hypertension: 27/90 ($p<0.001$);	single: 16.7% two: 26.7% ≥three: 56.7%
Diabetes mellitus: 14/46.7 ($p=0.855$);	
Obesity: 4/13.3 ($p<0.001$);	
Smoking: 15/50.0 ($p=1.0$);	
Alcohol abuse: 2/6.7 ($p<0.001$);	
Heart disease: 11/36.7 ($p=0.201$)	
Total: 100% ($p=0.001$)	100% ($p=0.001$)

vessel disease were the most frequent causes of these changes and the consecutive ischemic lesions.

Dimensions

The infarctions averaged 13.1×10.0 mm in diameter, and their mean surface area was 158.77 mm^2 . The paramedian lesions had the largest surface area (Table 2). Several positions of the lesions can be distinguished (Table 2). Each type of infarction will be illustrated by one or several clinical cases.

Paramedian infarctions

These infarctions (PMIs) comprised 30% of all ischemic pontine types (Table 2). We distinguished the complete, incomplete, and partial paramedian lesions.

The complete paramedian ischemic areas (Table 2) extended along the entire raphe pontis (Figs. 3B and 6A1). Due to that, the ischemic region damaged the pyramidal, corticobulbar, pontocerebellar and tectospinal tracts, the medial lemniscus and the medial longitudinal fasciculus (MLF), as well as the abducent nucleus, the genu of the facial nerve, and the horizontal gaze "center," i.e. the paramedian pontine reticular formation (PPRF) in the lower pons. In addition to some similar structures in the middle pons, the trigeminothalamic tract was also affected (Fig. 4B), as well as the rubrospinal tract, and partially the central tegmental tract and the locus coeruleus in the rostral pons (Fig. 5B)

Accordingly, the patient presented in Fig. 6A1 showed a left-side hemiparesis with arm predominance, dysarthria, ataxia, vomiting, and a disorder of the touch, the proprioceptive and vibration sense. Nystagmus, gaze

Table 2. Characteristics of the pontine infarctions

Affected part of the pons: % (p=)	Side: % (p=)	Infarction surface area of the main types: min-max (mean±SD) (p=)	Main infarction types: n/% (p=)	Infarction subtypes: n/% (p=)
Lower pons: 23.3; Middle pons: 10.0; Upper pons: 26.7; Lower & middle pons: 6.7; Middle & upper pons: 26.7; Lower, middle & upper pons: 6.7	Right: 43.4; Left: 46.7; Bilateral: 10,0	30-327 mm ² (163.11±108.57 mm ²) 8.3-131 mm ² (68.14±38.13 mm ²) 19-52 mm ² (29±13.58 mm ²) 32-666 mm ² (297±210.42 mm ²)	Paramedian: 9/30 Anterolateral: 8/26.7 Lateral: 6/20.0 Combined: 7/23.3	Paramedian complete: 2/6.7; Paramedian incomplete: 3/10.0; Anteromedial: 2/6.7; Posterior paramedian: 1/3.3; Paramedian paraventricular: 1/3.3 Anterolateral: 8/26.7 Lateral peripheral: 2/6.7; Centrolateral: 1/3.3; Posterolateral: 2/6.7; Lateral paraventricular: 1/3.3 Anteromedial & anterolateral: 3/10.0; Paramedian, anterolateral & lateral: 4/13.3
Total: 100% (p=0.001)	100% (p=0.002)	8.3-666.0 (158.8 mm ²) (p=0.031)	30/100% (p=0.690)	30/100% (p=0.157)

disturbances, internuclear ophthalmoplegia, and peripheral facial paresis were also present.

Certain ischemic lesions affected the paramedian region from the basis pontis to the posterior tegmentum (Fig. 6A–C). Accordingly, such lesions were classified as incomplete PMIs (Table 2). The presented patient showed hemiparesis (a lesion of the pyramidal fascicles), dysarthria and supranuclear facial paresis (damage to certain corticobulbar fibers), and slight signs of the medial lemniscus damage.

Among the partial PMI, the anteromedial lesion was seen in two patients (Table 2). In one of them, it was located at the pontomedullary junction (Fig. 7) and associated with mild right pure hemiparesis and supranuclear facial paresis, due to a lesion of the pyramidal and corticobulbar tracts. A circumscribed posterior paramedian ischemic lesion in another patient ((Fig. 8) displayed vertigo, nystagmus, vomiting and slight dysmetria (mainly due to damage of the pontocerebellar and vestibulocerebellar fibers), mild opposite proprioceptive disorder (a lesion of the medial lemniscus), and dysesthesia over the face (the affected trigeminothalamic tract).

Finally, a paramedian paraventricular infarction of the lower pons appeared in another patient (Fig. 9). He showed a left gaze paresis and deviation (a lesion of the abducent nucleus and the PPRF), including internuclear ophthalmoplegia (a lesion of the MLF), and ipsilateral peripheral facial paresis (damage to the facial nerve genu) (Fig. 3B). All the mentioned subtypes of the PMIs are presented in Figs. 10A1 and B1.

Anterolateral infarctions

The anterolateral lesions (Table 2) can extend to the level of the medial lemniscus (Figs. 4B, 5B, and 10C1). Among them, one patient had an isolated anterolateral infarction of the rostral pons (Fig. 11), and manifested mild hemiparesis (a lesion of the lateral part of the pyramidal tract), supranuclear facial paresis (damage to some corticobulbar fibers), and slight ataxia (a lesion of the cortico-ponto-cerebellar system).

A similar but smaller ischemic lesion was observed in several patients. Thus, one of them presented three small acute lacunar infarctions in the anterolateral pontine

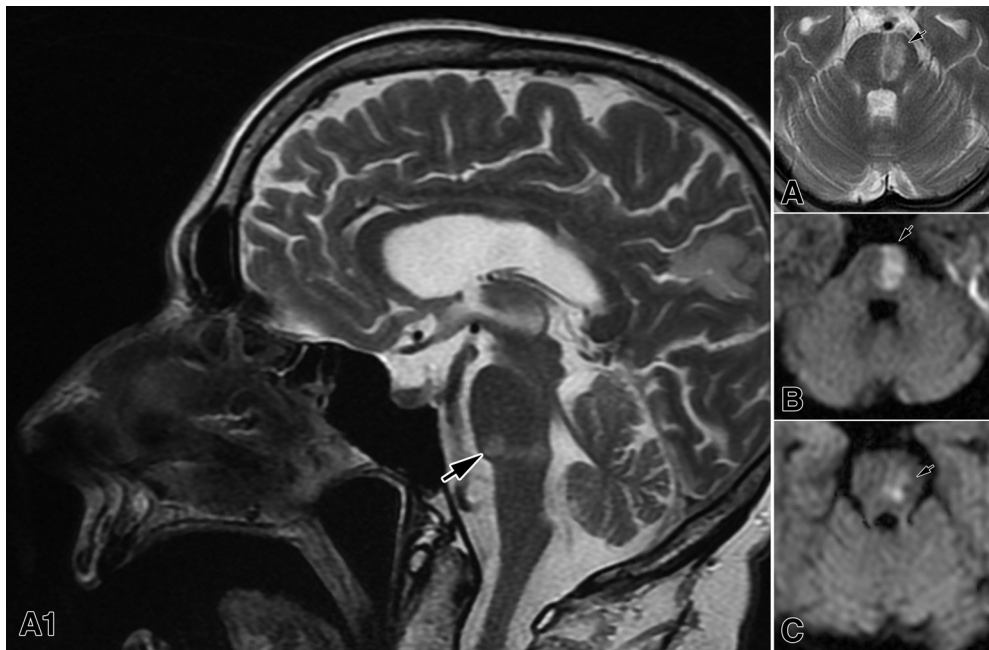


Fig. 6. A complete paramedian infarction of a patient (A1) close to the medulla oblongata in a sagittal T2-weighted section. Note a large left incomplete paramedian infarction (arrow) in T2-weighted (A) and DWI axial images (B and C) in another patient

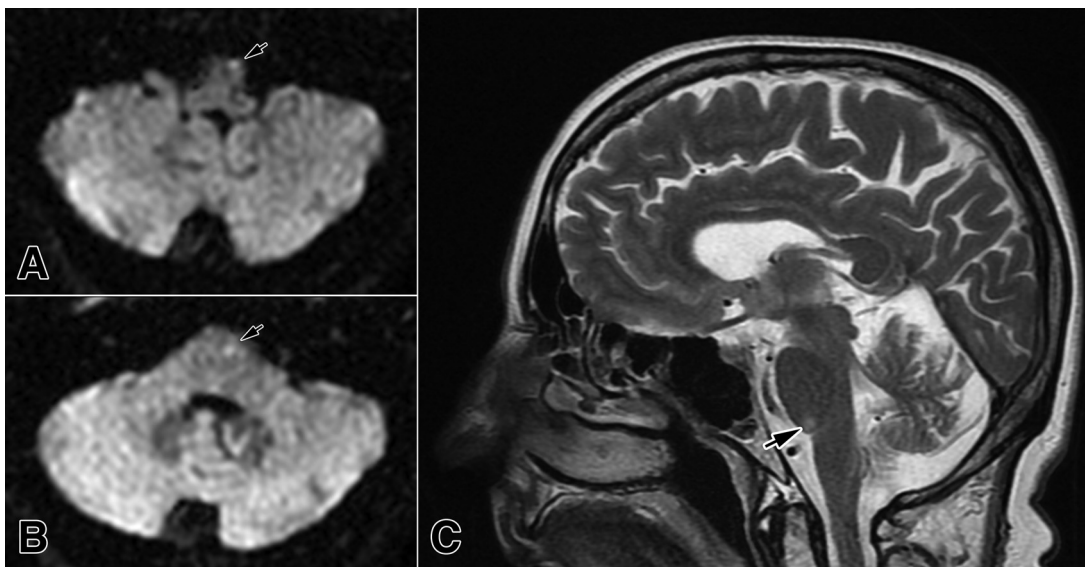


Fig. 7. A small left anteromedial pontomedullary infarction (arrows) in axial DWI sequences (A and B), and in a T2-weighted sagittal MRI image (C). The MRI was performed 6 days after onset

region (Fig. 12B), associated with a small old lesion in the same region of the lower pons (Fig. 12A), and by hypoplasia of the right vertebral artery (Fig. 12C).

Lateral infarctions

Isolated lateral ischemic lesions were present in 20% (Figs. 10A1 and C1). Among them, two were seen in the most peripheral part of the pons ("G" in Fig. 10C1). In one of these patients (Fig. 13), the ischemic lesion affected the

most lateral pyramidal and corticobulbar fascicles, the corticopontine and pontocerebellar fibers, as well as the middle cerebellar peduncle, causing mild hemiparesis, dysarthria, ataxia, gait disturbance, and vertigo.

Another patient showed a centrolateral infarction situated in the middle of the lateral region ("H" in Fig. 10C1). Two other patients had a posterolateral infarction ("I" in Fig. 10C1). One of them (Fig. 14) showed a damage to the central tegmental tract, pontocerebellar fibers, lateral lemniscus, and parts of the medial lemniscus, spinothalamic

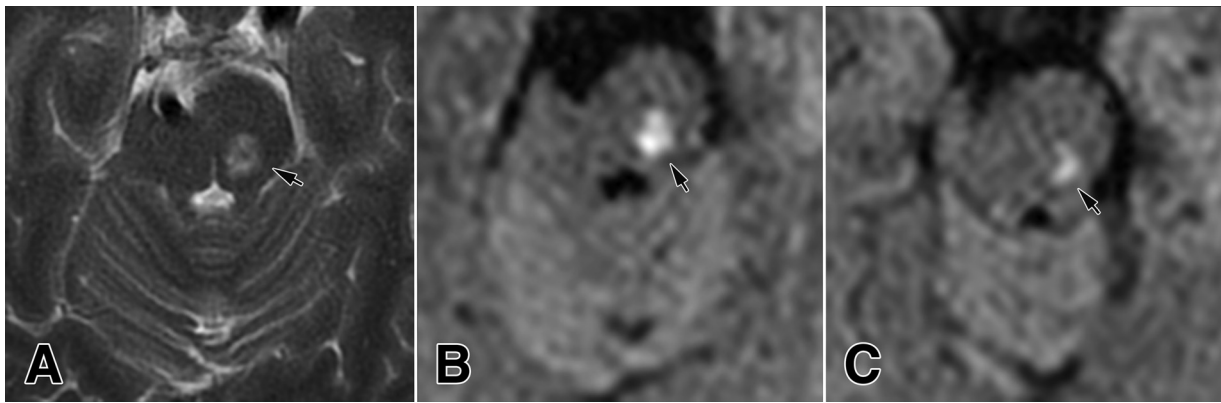


Fig. 8. A left posterior paramedian infarction (arrow) in a T2-weighted axial MRI image (A) and in DWI axial sequences (B and C) of the middle and rostral pons

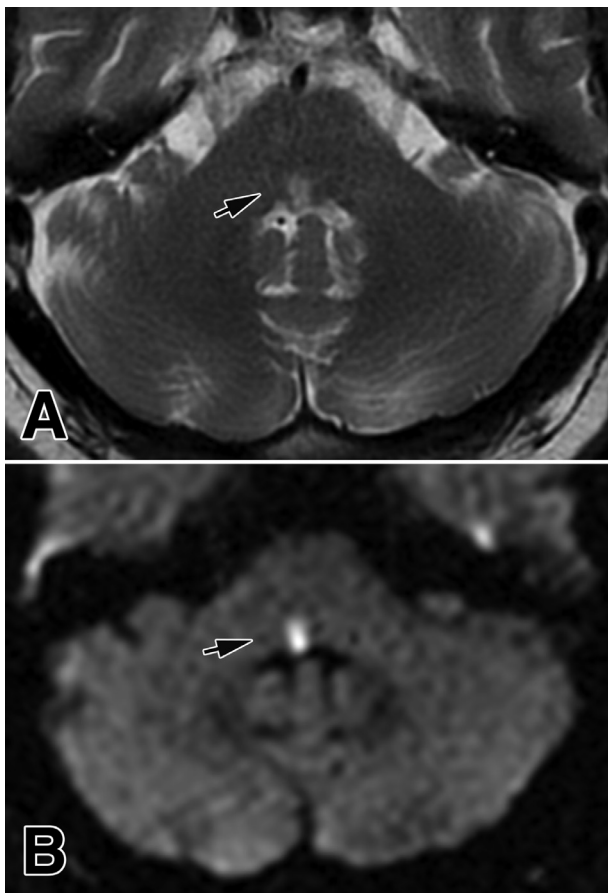


Fig. 9. A paramedian paraventricular ischemic lesion (arrows) in T2-weighted MRI (A) and DWI axial images (B)

and trigeminothalamic tracts. Consequently, the patient manifested gait unsteadiness, vertigo, and mild contralateral hemidysesthesia over the body and the face.

Finally, one patient showed a small isolated ischemic lesion in the lateral part of the posterior tegmentum (Fig. 15). This lateral paraventricular infarction mainly affected the vestibular nuclei (Figs. 3B and 10A1), and thus produced vertigo, vomiting, nystagmus, and gait unsteadiness.

Posterior infarctions

The two mentioned paramedian and lateral paraventricular lesions were the only isolated posterior tegmental damages we have observed. As for the rostral posterolateral tegmentum, which is supplied by the SCA branches (Figs. 4B and 5B), no infarction was found there.

Combined pontine infarctions

Combinations of some types of the presented PIs can be diagnosed in certain patients (Table 2).

Infarctions in 3 patients affected both the anteromedial and anterolateral pontine regions, including the pontomedullary junction. One of them, with a lesion of the pyramidal, corticobulbar and pontocerebellar fascicles, manifested headache, pure hemiparesis, supranuclear facial paresis, slight dysarthria, vomiting and confusion. Another patient also showed such an ischemic combination in the lower pons. The third patient manifested, among others, a poststroke depressive disorder.

The paramedian, anterolateral, and a part of the lateral vascular region were occasionally affected together (Table 2). The infarction in one patient, which occupied the pyramidal, corticobulbar and rubrospinal tracts, including a partial damage to the lateral lemniscus and the spinothalamic tract, manifested right hemiparesis, supranuclear facial palsy, dysarthria, and hemidysesthesia.

An infarction in another patient (Fig. 16), occupied the paramedian region, the anterolateral area, and most of the lateral pontine region. Mainly the pyramidal, corticobulbar and tectospinal tracts were damaged, as well as the PPRF, abducent nucleus, MLF, pontocerebellar fibers, medial and lateral lemnisci, as well as the spinothalamic tract. Hence, this patient manifested right hemiplegia, ataxia, facial paresis, gaze disturbances, hypoacusia, vertigo, lemniscal signs, and hemihypesthesia over the face and the body. A BA occlusion (Fig. 16F) was responsible for the infarction.

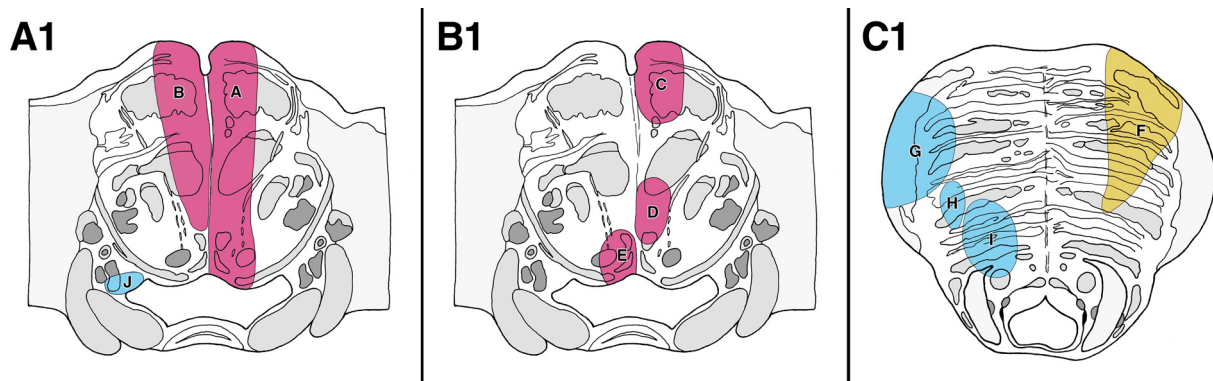


Fig. 10. A schematic presentation of infarction types in the caudal (A1 and B1) and the rostral pons (C1). Note a complete (A) and incomplete paramedian infarction (B), anteromedial (C), posterior paramedian (D) and paramedian paraventricular ischemic lesions (E), anterolateral (F), peripheral lateral (G), centromedian (H), posterolateral (I), and lateral paraventricular infarctions (J)

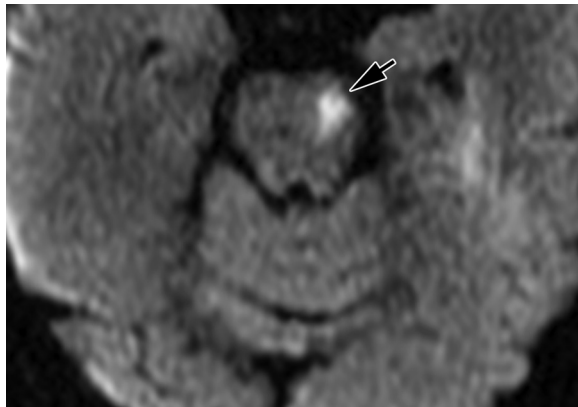


Fig. 11. An isolated acute left anterolateral infarction (arrow) in a DWI axial image of the rostral pons. (Compare with Figs. 5C and 10C1F)

Bilateral infarctions

These infarctions were observed in 3 patients (Table 2). In one of them, a unilateral acute ischemic lesion affected the left paramedian, anterolateral, and most of the lateral region, associated with a smaller contralateral lesion. The MRA presented multiple stenosis of a small right vertebral artery and an angulation of the BA distal segment. This patient manifested right hemiplegia, supranuclear facial

palsy, ataxia, dysarthria, hypoacusia, and medial lemniscal signs. The second patient was comparable to the first.

The infarction in the third patient occupied most of the pons, and a part of the right cerebellar hemisphere (Fig. 17) in the SCA territory. The patient manifested left-side hemiplegia and opposite hemiparesis, and various sensory, vestibular, supranuclear, and ocular signs. A BA dissection was present, as well as occlusion of the right ICA and the subclavian artery.

The involvement of the pontine and other structures

A recent infarction was associated with a small old ischemic lesion in the pons in only one patient (Fig. 12). An additional acute ischemic lesion in the cerebellum (Fig. 17A and B) was seen in 10% of the patients.

Discussion

PIs account for only about 7% of all IS according to radiologic studies,^{1,2,7,8} and for 9% of all lacunar infarctions in a pathologic examination.¹⁵ The main goal of this study was a comparison of the anatomic, radiologic and clinical data in these events. Whilst anatomic examination of the vascular territories and pathologic studies of

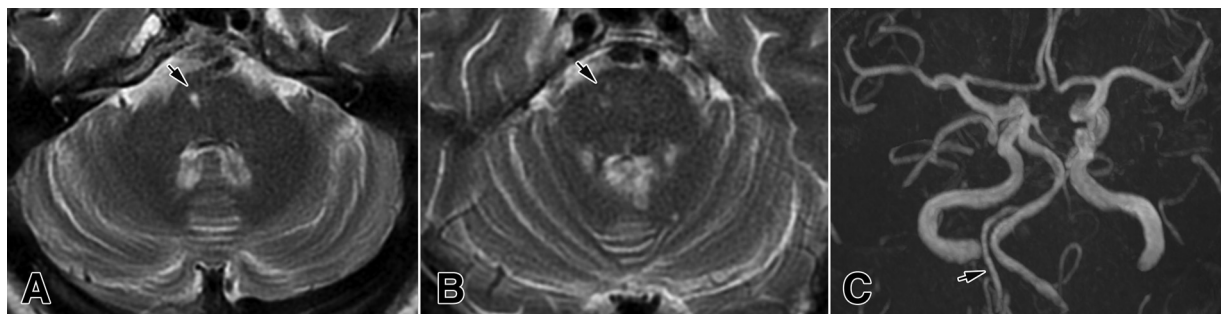


Fig. 12. A right old lacunar lesion (arrow) in a T2-weighted axial MRI image of the lower pons (A), and recent right small anterolateral lacunar infarctions (arrow) in a T2-weighted axial MRI image of the middle pons (B). Note a small right vertebral artery (arrow), an elongated, tortuous and locally stenotic basilar artery, as well as dilatation and atherosclerotic changes of both carotid arteries in the MRA-3D TOF image (C)

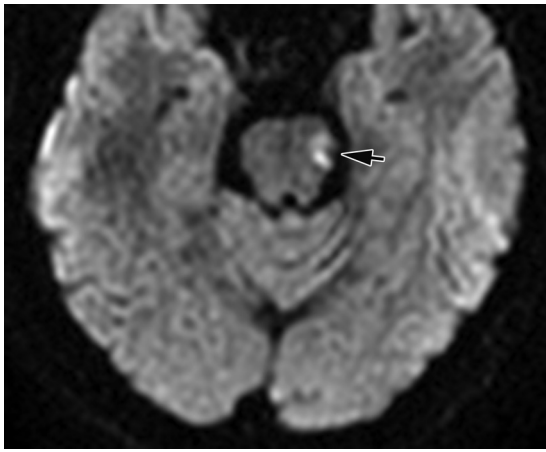


Fig. 13. An isolated acute left lateral infarction (arrow) in the peripheral part of the rostral pons, which partially affects the anterolateral region, presented in a DWI axial image

ischemic lesions are rare,^{3,10,12,15} radiologic reports are more frequent.^{1,4,5,7,9,16–20}

Infarction characteristics

Small lacunar infarctions can develop,^{3,4,6} but also large ischemic lesions involving most of the pons.^{4,5,7,18–20} A severe stenosis or occlusion of one or both the VAs, ICAs, BA, CCAs or subclavian artery were present in 86.7% of our patients. They can result in severe hemodynamic disorders, including blood steal, with a consequent hypoperfusion of the brain stem.²¹

Infarction diameters in our patients averaged 13.1×10.0 mm, and their surface area was 158.8 mm^2 .

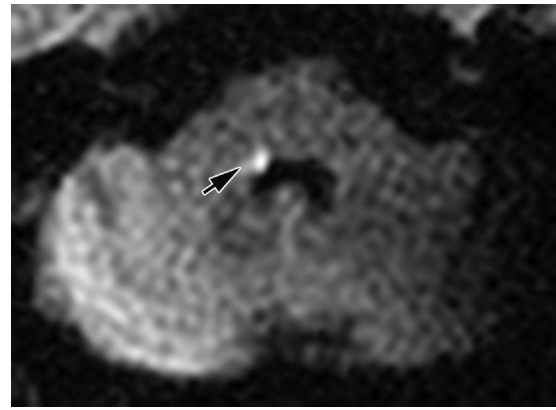


Fig. 15. A small right lateral paraventricular infarction (arrow) close to the corner of the 4th ventricle in a DWI image

The caudal, middle and rostral pons were involved in 23.3%, 10% and 26.7%, respectively (Table 2), which is somewhat different from the data in certain reports: 24.4–34.3%, 27.1–32.7% and 16.3–33.2%.^{1,7} Some others distinguished the basal, tegmental, and basotegmental infarctions,¹⁶ and certain other types.^{19,20} Our division is similar to a few other publications.^{2,8,12,21}

Infarction types

We distinguished the paramedian, anterolateral, lateral, posterior, combined, and bilateral ischemic lesions.

Paramedian infarctions

These infarctions (Fig. 6A1) are caused by an occlusion of the long paramedian branches of the perforating arteries.

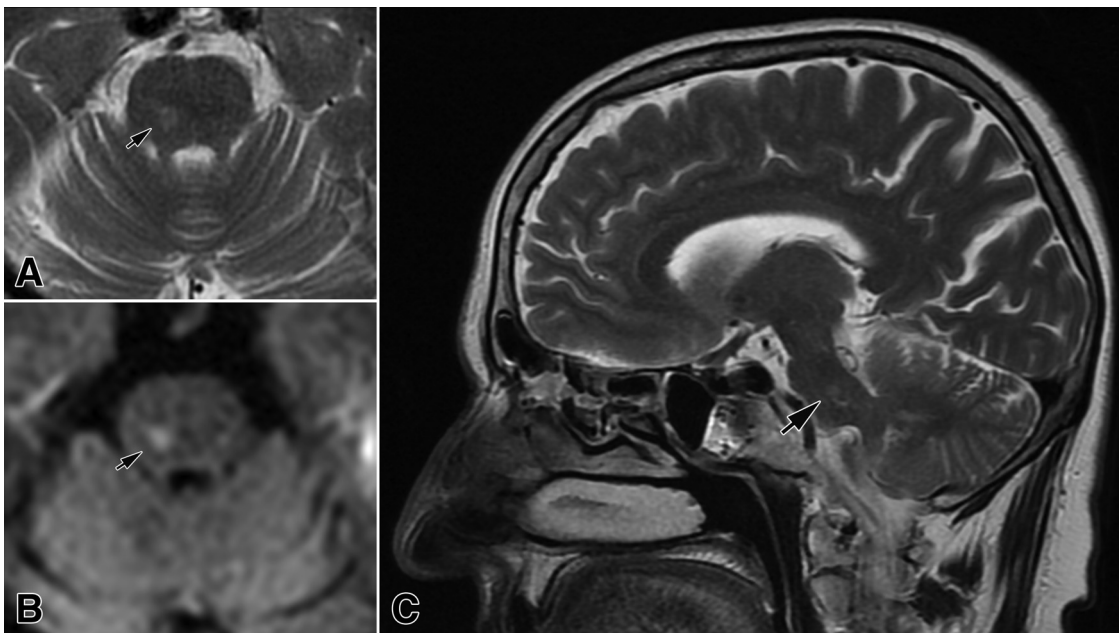


Fig. 14. A right posterolateral ischemic lesion (arrows) of the middle pons in axial T2-weighted (A) and DWI images (B), and in a T2-weighted sagittal image (C). The MRI was performed 5 days after onset

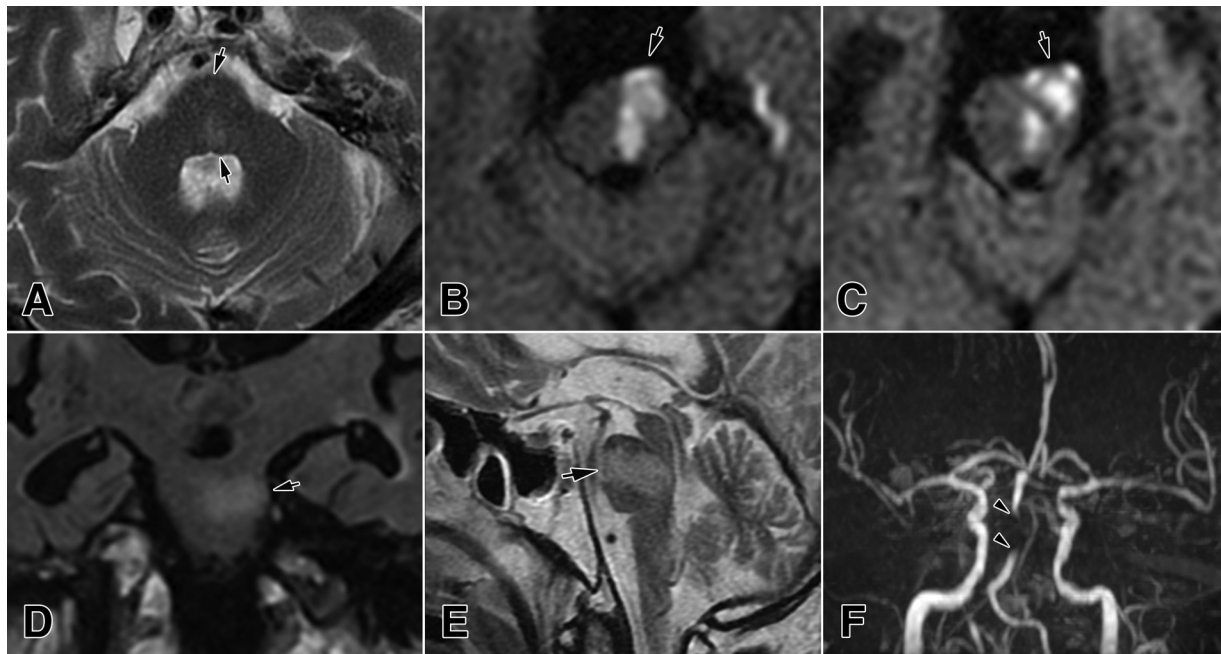


Fig. 16. A massive acute unilateral infarction (arrows) of the middle pons, and partially of the lower and upper pons (A through E) presented in T2-weighted MRI (A) and DWI axial images (B and C). Also note a FLAIR coronal image (D) and a T2-weighted MRI sagittal image (E), as well as occlusion of the basilar artery (between the two arrows) in a MRA-3D TOF image (F)



Fig. 17. A massive acute bilateral infarction (arrow) of the lower (A), middle (B) and rostral pons (C), and of the right cerebellar hemisphere (asterisk) shown in T2-weighted MRI (A and B) and DWI axial images (C), in a patient with a BA dissection, and an occlusion of the right ICA and the subclavian artery (not presented)

They account for 30% of the PIs in our study, compared with other results ranging from 28.3% to 73%.^{2,16–18,22}

The most characteristic sign in these patients was, first, hemiparesis (due to a lesion of the ventromedial pyramidal fascicles), either as pure motor or ataxic hemiparesis,^{3,6–8,21–23} which is sometimes associated with clumsy hand syndrome, dysarthria and dysphagia, and very rarely with a peripheral facial paresis, one-and-a-half syndrome, or pathologic crying or laughter.^{3,4,18,21,24} Hemiparesis in a complete paramedian lesion of the lower pons is often associated with facial paresis, or supranuclear lingual or palatal palsy, including dysarthria and rarely dysphagia (damage to certain corticobulbar fascicles), ataxia (lesion of the pontine nuclei, and corticopontine or pontocerebellar fibers), vertigo (lesion of the pontocerebellar fibers or

the vestibular nuclei), lemniscal signs, gaze disturbances (caused by a lesion of the horizontal gaze center and abducent nucleus), and internuclear ophthalmoplegia (lesion of the MLF).^{3,8,21,23}

Paramedian ischemia in the middle pons, where pyramidal bundles are not compact (Fig. 4B), can cause hemiparesis with arm predominance or brachial monoparesis, due to a lesion of the ventromedial pyramidal fascicles for hand and arm.^{18,25} Some supranuclear paresis also may appear.^{22,26} Contralateral face hemihypesthesia, eye pain, and gustatory disorders sometimes occur as a result of a lesion of the ventral trigeminothalamic decussation.²⁷ Damage to the cortico-ponto-cerebellar system causes ataxia.²¹ Lesion of the tectospinal tract can result in truncal ataxia and cervical dystonia.²⁸ It is a similar situation in the rostral pons (Fig. 5B).

In the case of incomplete paramedian infarctions (10%), there is occlusion of some shorter paramedian vessels.¹² In any case, hemiparesis, supranuclear nerve palsy, ataxia and nystagmus most often appear in these patients.

When only the anteromedial twig(s) of a PerfA are occluded, a larger or smaller anteromedial infarction develops (Fig. 7). It involves the medial pyramidal and corticobulbar fascicles, resulting in pure motor hemiparesis with arm predominance,^{18,25} and supranuclear palsy of some cranial nerves.^{2,20,21}

If only distal parts of certain paramedian arteries are occluded, a posteromedian infarction develops. When occlusion affects the terminal twigs of the longest paramedian arteries, a paramedian paraventricular tegmental lesion occurs¹⁸ (Fig. 9).

Anterolateral infarctions

Occlusion of an anterolateral artery, which appeared in 26.7% of our patients, and in 14% to 17% in some other reports,^{2,22} may result in a larger infarction extending to the level of the medial lemniscus. Small lacunar lesions are also possible in this region. Such lesions can result in hemiparesis with leg predominance (caused by damage to the leg and foot fascicles), some supranuclear nerve paresis, and ataxia.^{21,25,26}

Lateral infarctions

Lateral infarctions were diagnosed in 20% of our patients, and in 3% to 14% by some other authors.^{2,4} When a single shorter lateral artery is affected, or a side branch of a longer artery, an isolated peripheral lateral lesion will appear. In the case of a long branch occlusion within the lower pons (Fig. 3B), this can cause hemihypesthesia over the body (due to a lesion of the spinothalamic tract) and the face (damage to the spinal trigeminal nucleus and tract), hypoacusia (a lesion of the trapezoid body or lateral lemniscus), peripheral facial palsy (damage to the facial nucleus and fibers), some cardiovascular, respiratory and gustatory disorders (lesion of the solitary nucleus), palatal, pharyngeal, and vocal cords myoclonus (damage to the central tegmental tract), Horner's syndrome (damage to descending sympathetic fibers), and sometimes vestibular signs, due to a lesion of the vestibular nuclei or of the pontocerebellar fibers.^{21,26,29–31} The described ischemia is frequently caused by the AICA occlusion.³¹

If such an infarction affects the middle pons, some similar symptoms can appear, with the addition of masticatory muscles paresis (lesion of the motor trigeminal nucleus), facial hypesthesia (damage to the principal trigeminal nucleus), hypogeusia (lesion of the ascending gustatory fascicle), and sleep or behavior disorder in some patients, mainly due to a lesion of the locus coeruleus^{32–34} (Fig. 4B).

The location of a lateral infarct in the rostral pons (Fig. 5B) can result in mild hemiparesis with leg predominance (damage to the most lateral pyramidal fascicles), lemniscal signs, and sometimes hemihypesthesia for pain and temperature over the body (damage to the spinothalamic tract) or over the face (lesion of the trigeminothalamic tract).^{4,21}

Occlusion of terminal twigs of a longer lateral artery will cause a centrolateral or a posterolateral local ischemia (Figs. 10C1 and 14). Ataxia can appear, with the occasional addition of the medial lemniscus and the central tegmental tract lesions.^{21,29} A lateral tegmental paraventricular ischemia (Fig. 15) is associated with vertigo, vomiting, nystagmus, and gait unsteadiness, due to a vestibular nuclei lesion.³¹

As regards the mentioned consciousness and behavioral disorders, they are sometimes described as confusion, lethargy, loss of consciousness, disorientation, sleep disturbance, depression, bipolar disorder, and some psychotic manifestations.^{32–34} They are mainly a result of damage to the ascending reticular activating system, and certain neurotransmitter systems, including the norepinephrine nucleus locus coeruleus.³⁴ In addition, a rare occurrence of pathologic crying or laughter is a result of lesions of the corticobulbar emotional fibers and the pontine serotonergic system.^{35,36}

Posterior infarctions

The posterior tegmental region was rarely affected in our patients (6.7%), whilst a lesion of the posterolateral tegmental region of the rostral pons, supplied by the SCA branches, was not observed (Fig. 5B). According to Kobayashi et al.,² a dorsal infarction accounts for only 10%.

Combined infarctions

Combined lesions were noted in 23.3% of our patients. A common anteromedial and anterolateral ischemic lesion was already described. A combination of the paramedian, anterolateral and lateral infarctions can appear as a result of large artery disease.^{6,21} Bilateral infarctions (Fig. 17) were present in 10% of our patients, which is similar (7.4–11%) to other reports.^{20,21} Such lesions are accompanied by many symptoms and signs, including occasionally loss of consciousness and locked-in-syndrome.^{20,37}

Some bilateral infarctions occupy only the anterior (ventral) basis pontis (in 4%).²⁰ They are commonly associated with tetraplegia, pseudobulbar palsy, and occasionally loss of consciousness. In some other patients, a bilateral tegmental (paraventricular) ischemia occurred, which was associated with a bilateral horizontal gaze and facial paresis in the lower pons.²¹

Radiologic and clinical implications of the anatomic findings

The anatomic fact that the PerfAs often give rise to the anterolateral branches means that a PerfA occlusion can lead to a combined paramedian and anterolateral infarction, which was observed in 26.7% of our patients. An occlusion of a common stem of the PerfAs themselves (Fig. 2) can result in a longer PMI affecting one or two vertical pontine segments. Their common origin with a longer pontine artery can produce a combined paramedian, anterolateral, and lateral infarction.

It is a similar situation in the case of the AICA or SCA occlusion which can give rise to a PerfA or the ALAs. A specimen with a PerfA supplying both sides of the pons is the basis for a bilateral infarction occurrence. In another specimen, a PerfA, as well as all the PMAs, took part in the nourishing of both the lower pons and the upper medulla, which can explain the appearance of infarctions at the pontomedullary junction.

The extent of an infarction also depends on the presence and size of the anastomotic channels,¹⁰ which were seen among the ILPA and SLPA in 56.3% of the specimens. The second factors are the BA atherosclerosis and small vessels disease of certain intrapontine arteries, which can compromise the blood flow through the BA branches.^{1–8}

The mentioned anatomic features can cause certain vascular and territorial variability.^{10–12} Vascular variability mainly refers to a various origin, number and diameter of the pontine arteries. In general, if there are a smaller number of the vessels in a certain group, e.g. the perforating arteries, these vessels are larger in diameter. Similarly, the smaller the vessels size, the larger their diameter. Also, if an artery arises by a common stem with another artery, a larger supplying region appears. Finally, when an artery is missing, e.g. the pontomedullary or the posterolateral pontine artery, its region of supply is taken over by the adjacent vessels.

The mentioned facts have direct implications regarding the size of a vascular territory.^{10–12} Thus, larger pontine arteries, due to their larger diameter and ramification zone, supply a larger part of the pontine parenchyma. It is the reverse situation in the case of a smaller size of the same arteries. As a consequence, some intrapontine structures, which are usually nourished by a certain artery in most of the cases, can be occasionally supplied by an adjacent vessel, either partially or completely.

For example, the abducent nucleus is vascularized by the paramedian arteries, but with the addition of the AICA twigs in some cases (Fig. 3B). The vestibular nuclei can be nourished by the latter twigs, but occasionally also by the SCA dorsal branches¹⁰. The latter branches in the upper pons most often supply the lateral lemniscus, the superior cerebellar peduncle, and the mesencephalic trigeminal nucleus and tract (Fig. 5B), but also the entire locus coeruleus and the central tegmental tract in some cases.

It means that the main vascular territories can be larger or smaller in certain cases, depending on the origin, diameter, and branching patterns of the pontine arteries. Consequently, our templates (Figs. 3 through 5) are a presentation of the averaged regions of supply, based on our and others' examination.^{10–12} This is why there is occasionally some mismatch of a drawn vascular region and an infarction in the same region. For instance, the incomplete paramedian infarction in Fig. 5ABC is larger than expected as compared to Figs. 3 and 5, since the paramedian arteries most likely supplied a larger region than usual. It is the same case with the partial paramedian ischemic area in Fig. 8.

Such individual examples can be completely and reliably examined only by applying ultrahigh field MRI, e.g. 7 or 9 Tesla, and by the increase of computational power, which enable a visual presentation of the small intraparenchymal arteries.³⁸

Conclusions

The pontine structures are supplied by the perforating arteries, with their paramedian and anteromedial branches, the anterolateral, lateral and posterior vessels. Hence, pontine infarctions were divided into the complete (6.7%), incomplete (10%) and partial paramedian (13.3%), anterolateral (26.7%), lateral (20%), and posterior (6.7%) lesions, as well as into their various combinations (23.3%).

Funding

This research received no specific grant from any funding agency in the public, commercial, or not-for-profit sectors.

Declaration of Competing Interest

None

References

- Oh S, Bang OY, Chung CS, Lee KH, Chang WH, Kim GM. Topographic location of acute pontine infarction is associated with the development of progressive motor deficits. *Stroke* 2012;43:708-713. <https://doi.org/10.1161/STROKEAHA.111.632307>.
- Kobayashi J, Bomoyuki O, Minematsu K, Nagatsuka K, Toyoda K. Etiological mechanisms of isolated pontine infarcts based on arterial territory involvement. *J Neurol Sci*. 2014;339:113-117. <https://doi.org/10.1016/j.jns.2014.01.039>.
- Fisher CM. Lacunar strokes and infarcts: A review. *Neurology (Ny)* 1982;32:871-876.
- Kataoka S, Miaki M, Saiki M, Saiki S, Yamaya Y, Hori A, Hirose G. Rostral lateral pontine infarction. Neurological/topographical correlations. *Neurology* 2003;61:114-117. <https://doi.org/10.1212/01.WNL.0000072323.19180.B7>.
- Xia C, Chen HS, Wu SW, Xu WH. Etiology of isolated pontine infarctions: a study based on high-resolution

- MRI and brain small vessel disease scores. *BMC Neurol* 2017;17:216. <https://doi.org/10.1186/s12883-017-0999-7>.
6. Klein IF, Lavalle PC, Mazaighi M, Schouman-Claeys E, Labreuche J, Amarenco P. Basilar artery atherosclerotic plaques in paramedian and lacunar pontine infarctions. A high/resolution MRI study. *Stroke* 2010;41:1405-1409. <https://doi.org/10.1161/STROKEAHA.110.583534>.
 7. Kim JS, Lee JH, Im JH, Lee MC. Syndromes of pontine base infarction. A clinical-radiological correlation study. *Stroke* 1995;26:950-955. <https://doi.org/10.1161/01.26.6.950>.
 8. Salerno A, Strambo D, Nannoni S, Dunet V, Michel P. Patterns of ischemic posterior circulation strokes: A clinical, anatomical, and radiological review. *Int J Stroke* 2021;0:1-9. <https://doi.org/10.1177/17474930211046758>.
 9. Huang R, Zhang X, Chen W, Lin J, Chai Z, Yi X. Stroke subtypes and topographic locations associated with neurological deterioration in acute isolated pontine infarction. *J Stroke Cerebrovasc Dis* 2016;25:206-213. <https://doi.org/10.1016/j.jstrokecerebrovasdis.2015.09.019>.
 10. Duvernoy HM. *Human Brainstem Vessels*. Berlin: Springer-Verlag; 1978.
 11. Marinković S, Gibo H. The surgical anatomy of the perforating branches of the basilar artery. *Neurosurgery* 1993;33:80-87. <https://doi.org/10.1227/00006123-199307000-00012>.
 12. Tatu L, Moulin T, Bogousslavsky J, Duvernoy H. Arterial territories of human brain: brainstem and cerebellum. *Neurology* 1996;47:1125-1135. <https://doi.org/10.1212/WNL.47.5.1125>.
 13. Chan KK, Lowe J. *Techniques in neuropathology*. In: Bancroft JD, Gamble M, eds. *Theory and Practice of Histological Techniques*, London: Churchill Livingstone; 2002:271-320.
 14. Nieuwenhuys R, Voogd J, van Huijzen C. *The Human Central Nervous System. A Synopsis and Atlas*. Berlin: Springer-Verlag; 1988.
 15. Dozono K, Ishii N, Nishihara Y, Horie A. An autopsy study of the incidence of lacunes in relation to age, hypertension, and arteriosclerosis. *Stroke* 1991;22:993-996.
 16. Field TS, Benavente OR. Penetrating artery territory pontine infarction. *Rev Neurol Dis* 2011;8:30-38. <https://doi.org/10.3909/rind0277>.
 17. Bassetti C, Bogousslavsky J, Barth A, Regli F. Isolated infarcts of the pons. *Neurology* 1996;46:165-175. <https://doi.org/10.1212/WNL.46.1.165>. doi.org/.
 18. Kataoka S, Hori A, Shirakawa T, Hirose G. Paramedian pontine infarction. Neurological topographical correlation. *Stroke* 1997;28:809-815. <https://doi.org/10.1161/01.str.28.4.809>.
 19. Wilson LK, Pearce LA, Araz A, Anderson DC, Tapia J, Bazan C, Venavente OR, Field TS. Morphological classification of penetrating artery pontine infarcts and association with risk factors and prognosis: The SPS3 trial. *Int J Stroke* 2016;11:412-419. <https://doi.org/10.1177/1747493016637366>.
 20. Huang J, Qiu Z, Zhou P, Li J, Chen Y, Huang R, Li C, Ouyang X, Feng H, Xu H, et al. Topographic location of unisolated pontine infarction. *BMC Neurol* 2019;19:186-195. <https://doi.org/10.1186/s12883-019-1411-6>.
 21. Ropper AH, Samuels MA. *Adams and Victor's Principles of Neurology*. New York: McGraw Hill Medical; 2009.
 22. Kumral E, Bayülkem G, Evyapan D. Clinical spectrum of pontine infarction. *J Neurol* 2002;249:1659-1670. <https://doi.org/10.1007/s00415-002-0879-x>.
 23. Chang MC, Kwak SG, Chun MH. Dysphagia in patients with isolated pontine infarction. *Neural Regen Res* 2018;13:2156-2159. <https://doi.org/10.4103/1673-5374.241466>.
 24. Agarwal R, Manandhar L, Saluja P, Grandhi B. Pontine stroke presenting as isolated facial nerve palsy mimicking Bell's palsy: a case report. *J Med Case Rep* 2011;5:287-290. <http://www.jmedialcasereports/5/1/287>.
 25. Jang SH. Somatotopic arrangement and location of the corticospinal tract in the brainstem of the human brain. *Yonsei Med J* 2011;52:553-557. <https://doi.org/10.3349/ymj.52.4.553>.
 26. Jang S, Kim J, Seo Y, Kwak S. Recovery of an injured corticobulbar tract in a patient with stroke. A case report. *Medicine* 2017;96(38):e7636. <https://doi.org/10.1097/MD.0000000000007636>.
 27. Simon NG, Tisch S, Chaganti J, Markus R. Fluctuating gustatory disturbance and ophthalmodynia heralding the onset of a paramedian pontine infarction. *J Clin Neurosci* 2011;18:983-985. <https://doi.org/10.1016/j.jocn.2010.11.026>.
 28. McGovern EM, Killian O, Narasimham S, Quinlivan B, Butler JB, Beck R, Beiser I, Williams LW, Killeen RP, Farrell M, et al. Disrupted superior collicular activity may reveal cervical dystonia disease pathomechanisms. *Sci Rep* 2017;7:16753. <https://doi.org/10.1038/s41598-017-17074-x>.
 29. Shioda M, Hayashi M, Takanashi J, Osawa M. Lesions in the central tegmental tract in autopsy cases of developmental brain disorders. *Brain Develop* 2011;33:541-547. <https://doi.org/10.1016/j.braindev.2010.09.010>.
 30. Boscan P, Pickering AE, Paton JFR. The nucleus of the solitary tract: an integrating station for nociceptive and cardiorespiratory afferents. *Exp Physiol* 2002;87:259-266. <https://doi.org/10.1113/eph8702353>.
 31. Lee H. Audiovestibular loss in anterior inferior cerebellar artery territory infarction: a window to early detection? *J Neurol Sci* 2012;313:153-159. <https://doi.org/10.1016/j.jns.2011.08.039>.
 32. Xi Z, Luning W. REM sleep behavior disorder in a patient with pontine stroke. *Sleep Med* 2009;10:143-146. <https://doi.org/10.1016/j.sleep.2007.12.002>.
 33. Belli H, Akbudak M, Ural C, Kulacaoglu F. Solitary lesion in ponto-mesencephalic area related secondary mania: a case report. *Psychiat Danub* 2012;24:223-225.
 34. Grueschow M, Kleim B, Christian C, Ruff CC. Role of the locus coeruleus arousal system in cognitive control. *J Neuroendocrin* 2020;32:e12890. <https://doi.org/10.1111/jne.12890>.
 35. Elyas AE, Bulters DO, Sparrow OC. Pathological laughter and crying in patients with pontine lesions: Case report. *J Neurosurg Pediatr* 2011;8:544-547. <https://doi.org/10.3171/2011.8.PEDS11265>.
 36. Kameyama S, Masuda H, Shirozu H. Location of emotional corticobulbar tract in the internal capsule. *J Neurol Sci* 2021;410:117228. <https://doi.org/10.1016/j.jns.2020.117228>.
 37. Samaniego EA, Lansberg MG, DeGeorgia M, Venkatasubramanian C, Wijman CAC. Favorable outcome from a locked-in state despite extensive pontine infarction by MRI. *Neurocrit Care* 2009;11:369. <https://doi.org/10.1007/s12028-009-9268-y>.
 38. Zwanenburg JJM, van Osch MJP. Targeting cerebral small vessel disease with MRI. *Stroke* 2017;48:3175-3182. <https://doi.org/10.1161/STROKEAHA.117.016996>.